Clim Dyn (2013) 40:2381–2399
DOI 10.1007/s00382-012-1516-8

Initialisation and predictability of the AMOC over the last 50 years in a climate model

Didier Swingedouw · Juliette Mignot · Sonia Labetoulle · Eric Guilyardi · Gurvan Madec

Received: 6 November 2011 / Accepted: 1 August 2012 / Published online: 18 September 2012
© Springer-Verlag 2012

Abstract The mechanisms involved in Atlantic meridional overturning circulation (AMOC) decadal variability and predictability over the last 50 years are analysed in the IPSL–CM5A–LR model using historical and initialised simulations. The initialisation procedure only uses nudging towards sea surface temperature anomalies with a physically based restoring coefficient. When compared to two independent AMOC reconstructions, both the historical and nudged ensemble simulations exhibit skill at reproducing AMOC variations from 1977 onwards, and in particular two maxima occurring respectively around 1978 and 1997. We argue that one source of skill is related to the large Mount Agung volcanic eruption starting in 1963, which reset an internal 20-year variability cycle in the North Atlantic in the model. This cycle involves the East Greenland Current intensity, and advection of active tracers along the subpolar gyre, which leads to an AMOC maximum around 15 years after the Mount Agung eruption. The 1997 maximum occurs approximately 20 years after the former one. The nudged simulations better reproduce this second maximum than the historical simulations. This is due to the initialisation of a cooling of the convection sites in the 1980s under the effect of a persistent North Atlantic oscillation (NAO) positive phase, a feature not captured in the historical simulations. Hence we argue that the 20-year cycle excited by the 1963 Mount Agung eruption together with the NAO forcing both contributed to the 1990s AMOC maximum. These results support the existence of a 20-year cycle in the North Atlantic in the observations. Hindcasts following the CMIP5 protocol are launched from a nudged simulation every 5 years for the 1960–2005 period. They exhibit significant correlation skill score as compared to an independent reconstruction of the AMOC from 4-year lead-time average. This encouraging result is accompanied by increased correlation skills in reproducing the observed 2-m air temperature in the bordering regions of the North Atlantic as compared to non-initialized simulations. To a lesser extent, predicted precipitation tends to correlate with the nudged simulation in the tropical Atlantic. We argue that this skill is due to the initialisation and predictability of the AMOC in the present prediction system. The mechanisms evidenced here support the idea of volcanic eruptions as a pacemaker for internal variability of the AMOC. Together with the existence of a 20-year cycle in the North Atlantic they propose a novel and complementary explanation for the AMOC variations over the last 50 years.

Keywords Decadal climate prediction · Ocean dynamics · Atlantic meridional overturning circulation · Hindcast · Predictability · Volcanic eruptions · Mount Agung · North Atlantic oscillation

This paper is a contribution to the special issue on the IPSL and CNRM global climate and Earth System Models, both developed in France and contributing to the 5th coupled model intercomparison project.

D. Swingedouw (✉)
LSCE/IPSL, Gif-sur-Yvette, France
e-mail: swingedo@cerfacs.fr

J. Mignot · S. Labetoulle · E. Guilyardi · G. Madec
LOCEAN/IPSL, Paris, France

E. Guilyardi
NCAS-Climate, University of Reading, Reading, UK

G. Madec
NOCS, Southampton, UK

1 Introduction

One of the key hypothesis underlying decadal climate predictability involves ocean memory at this time scale. The ocean indeed has a larger thermal inertia than land areas, and observations suggest that it has enhanced variability at the decadal time scales (e.g. Deser and Blackmon 1993; Czaja and Marshall 2001; Álvarez-Garcia et al. 2008; Frankcombe et al. 2010). The prerequisite of decadal prediction is therefore to assimilate observations, and most importantly oceanic observations, in climate models in order to correctly initialise this climatic component.

So far, diagnostic predictability studies using climate models have shown that a few specific regions exhibit low frequency variability with amplitude similar to the interannual variability (Boer 2004). One of the most promising regions is the North Atlantic (Latif et al. 2006). This is thought to be due to the Atlantic meridional overturning circulation (AMOC), a large-scale oceanic circulation with a sinking branch in the North Atlantic, which has a strong influence on the heat transport and redistribution in the whole Atlantic basin. This circulation is notably thought to drive a large part of the Atlantic multi-decadal variability in sea surface temperature (SST) (Knight et al. 2005), with large influence on European temperatures (Latif et al. 2006) and on the India/Sahel rainfall and Atlantic hurricanes (Zhang and Delworth 2006). The AMOC has exhibited potential predictability in several climate models (e.g. Pohlmann et al. 2004; Collins et al. 2006; Msadek et al. 2010; Persechino et al. submitted). The working assumption is that correctly initialising the AMOC in a decadal climate system can provide predictability.

Both the characteristics (frequency, amplitude) and the processes responsible for AMOC variability are highly model-dependent. The main time scales for the AMOC variability in climate models range from 10 to 100 years. The mechanisms explaining the AMOC decadal variability vary from purely oceanic origins, forced by atmospheric noise (e.g. Dijkstra and Ghil 2005) to coupled ocean–atmosphere processes (Timmermann et al. 1998), with sea-ice processes possibly playing an active role (Escudier et al. submitted). In addition to internal variability, external forcing such as volcanic eruptions (Otterå et al. 2010; Iwi et al. 2012; Zanchettin et al. 2012) has been suggested to have a key role in the phasing of the AMOC cycle.

Direct observations of the AMOC are not available, so that a large uncertainty on past AMOC variations remains. Latif et al. (2004) proposed a reconstruction of the AMOC over the last few decades, using a dipole of SST between the Northern and Southern Atlantic. They found that the leading atmospheric variability mode on the North Atlantic, the North Atlantic oscillation (NAO), leads their AMOC index by around 10 years over the recent period. They explained such an influence by the impact of the NAO on the Labrador Sea convection in winter through the large heat flux that cools the ocean when the NAO is positive, leading to a decrease in surface density, which triggers a convective event (see also Eden and Jung 2001; Delworth and Greatbatch 2000).

A few attempts to measure present-day AMOC have been undertaken in the recent years (Cunningham et al. 2007; Lherminier et al. 2010). A reconstruction proposed by Huck et al. (2008) exhibits AMOC variations with local maxima around 1980 and in the mid-1990s, in agreement with oceanic reanalyses products (Köhl and Stammer 2008). Huck et al. (2008) mainly used in situ data at depth as well as observed surface fields, which may provide a more robust reconstruction than using only SST. Concerning the preferred frequency for SST variability in the Atlantic, Frankcombe et al. (2010), using coupled climate models as well as observed SST, proposed two dominant time scales: a 20–30 years scale caused by the AMOC internal variability and a 50–70 years scale related to atmospheric forcing over the Atlantic and exchange processes with the Arctic. Using the reconstructions from Greenlandic ice cores, Chylek et al. (2011) partly confirmed this time scale more recently, on a longer time frame. They showed two dominant time scales (20 and 45–85 years), but found that the only statistically significant one is the 20-year time scale. In the ocean, Sicre et al. (2008) found similar significant 20-year time scale in an oceanic core drilled north of Iceland and reconstructing 2,000 years of SST variability there.

In climate models, Tulloch and Marshall (2012) discussed this 20-year time scale for the North Atlantic variability, present in recent version of the NCAR and GFDL climate models. Such a frequency was also found as the most significant for variations of the AMOC and other oceanic fields in the subpolar North Atlantic in a 1,000-year preindustrial simulation using the IPSL–CM5A–LR climate model (Escudier et al. submitted), which is the same model as in the present study. The mechanism explaining such a variability was shown to be a cycle beginning (for instance) with an intensification of the East Greenland Current (EGC) that brings more cold and fresh water in the Labrador Sea where it accumulates and gives rise to negative SST and sea surface salinity (SSS) anomalies. These anomalies are advected along the subpolar gyre; they affect the convection all along their path up to the Nordics Seas, where the negative SST anomalies increase the sea-ice cover, which in turn induces a positive sea-level pressure anomaly and a localised anticyclonic atmospheric circulation. This leads to a decrease in the wind stress along the eastern coast of Greenland and thus a weakening of the EGC, conducing to an opposite phase of the cycle around 10 years after its initiation. The impact of

this cycle on the AMOC is made through the impact of SSS anomalies on the convective activity in the North Atlantic, which then influences the AMOC variations. Atmospheric noise plays a role in modulating notably the amplitude of the cycle, explaining that some cycles have larger magnitude than others.

The underlying assumption for decadal prediction is to suppose that the observed climate and oceanic decadal variability, at the source of potential predictability, is correctly represented in climate models. The goal is then to phase the model with the observed variability. In other words, in this approach, decadal prediction is an attempt to synchronise internal modes of variability of the model with the real world. This is the delicate "initialisation problem". A few attempts have already been made with different strategies; more are to come in the framework of the CMIP5 project (e.g. Taylor et al. 2012). Smith et al. (2008) used a three-dimensional (3D) oceanic reanalysis and surface temperature and pressure as restoring terms for their initialised simulation. They used anomalies for all the fields in order to avoid large drift from initial adjustment. Keenlyside et al. (2008) chose a simpler approach: they restored only towards the observed anomalous SST up to 60° of latitude in their coupled climate model. Nevertheless it appears that their experimental design leads to lower correlation with global observed temperature than a simple historical simulation using only external forcing, suggesting some limits in the experimental setup. More recently Pohlmann et al. (2009) and Dunstone and Smith (2010), using two different models initialised with different 3D oceanic reanalysis, found skills in initialising the North Atlantic sector and the AMOC. Finally, Zhang et al. (2009) propose an innovative initialisation technique, based on coupled data assimilation, which proved efficient up to interannual timescales.

In the present study we describe a new prediction system using the IPSL–CM5A–LR climate model and SST anomalies as the only restoring data (Sect. 2). The initialisation of the AMOC and the associated mechanisms, are presented in Sect. 3. We then evaluate the predictability of the system using decadal hindcasts (Sect. 4). A summary of the main results and a discussion conclude the paper (Sect. 5).

2 Experimental design

The ocean–atmosphere coupled model used in this study is the IPSL–CM5A (Dufresne et al. submitted) in its low-resolution (LR) version as developed for CMIP5. The atmospheric model is LMDZ5 (Hourdin et al. 2006) with a 96 × 96 × L39 regular grid and the oceanic model is NEMO (Madec 2008) with an 182 × 149 × L31 non-regular grid, in version 3.2, including the LIM-2 sea ice model (Fichefet and Maqueda 1997; Timmermann et al. 2005) and the PISCES module for oceanic biogeochemistry (Aumont and Bopp 2006). The internal variability of the AMOC in this model has been analysed in details in Escudier et al. (submitted).

The set of experiments that will be considered in the present study is summarised in Table 1. It first includes the five-member ensemble of *historical* simulations available in the CMIP5 database. These simulations use prescribed external radiative forcing from the observed increase in greenhouse gases and aerosol concentrations as well as the ozone changes (Fig. 1) and the land-use modifications (not shown, see Dufresne et al. submitted). They also include estimates of solar irradiance variations and volcanic eruptions represented as a decrease in the total solar irradiance (depending on the intensity of the volcanic eruption, Fig. 1). These historical simulations start from year 1850. Their initial conditions come from different dates of the 1,000-year control simulation under preindustrial conditions each separated by 10 years.

In order to separate the effect of anthropogenic forcing and natural one (red and black curves from Fig. 1 respectively), we additionally consider two ensembles of simulations each composed of three members and following a similar set up as the historical ones, but using either the anthropogenic (greenhouse gases, aerosols, ozone, land use) or the natural (solar and volcanic) forcing. They are respectively called *anthropogenic* and *natural* in the rest of the paper.

We also consider a five-member ensemble of *nudged* simulations, which include a nudging term towards observed anomalous SST variations. Each simulation starts on January 1st 1949 from one of the historical simulations presented above. Each nudged simulation is therefore associated with one historical simulation. These nudged simulations are using the same external forcing as the historical ones (Fig. 1). The nudging technique consists in adding a heat flux term Q to the SST equation under the form $Q = -\gamma(\mathrm{SST}'_{\mathrm{mod}} - \mathrm{SST}'_{\mathrm{obs}})$ where $\mathrm{SST}'_{\mathrm{mod}}$ stands for the modelled anomalous SST at each time step and grid point, and $\mathrm{SST}'_{\mathrm{obs}}$ the anomalous observed SST (Reynolds et al. 2007; Smith et al. 2008). Anomalies are computed with respect to the average SST over the period 1949–2005 in the corresponding historical simulation and in the observations respectively. We use a restoring coefficient γ of 40 W m^{-2}/K corresponding to a relaxing timescale of around 60 days (for a mixed layer of 50 m depth). This amplitude of γ was chosen from physically basis: it corresponds typically to air-sea thermal coupling magnitude as diagnosed in ocean-only general circulation models (GCMs) (Haney 1971; Madec and Delecluse 1997;

Table 1 Description of the simulations

	No. ensemble	Initial conditions	Forcing	Restoring	Years of simulation
Control	1	Spin-up simulation	Preindustrial	No	1 × 1,000
Historical	5	Start in 1850 every 10 years from a preindustrial simulation	Natural + anthropogenic	No	5 × 156
Nudged	5	Start in 1948 from each associated historical simulation	Natural + anthropogenic	SST anomalies from Reynolds et al. (2007)	5 × 57
Hindcast	3	Start every 5 years from the 1st Jan. 1961 from a nudged simulation plus a spatial white noise on SST	Natural + anthropogenic and RCP4.5	No	3 × 10 × 10
Natural	3	Start in 1850 every 10 years from a preindustrial simulation	Natural	No	3 × 156
Anthropogenic	3	Start in 1850 every 10 years from a preindustrial simulation	Anthropogenic	No	3 × 156

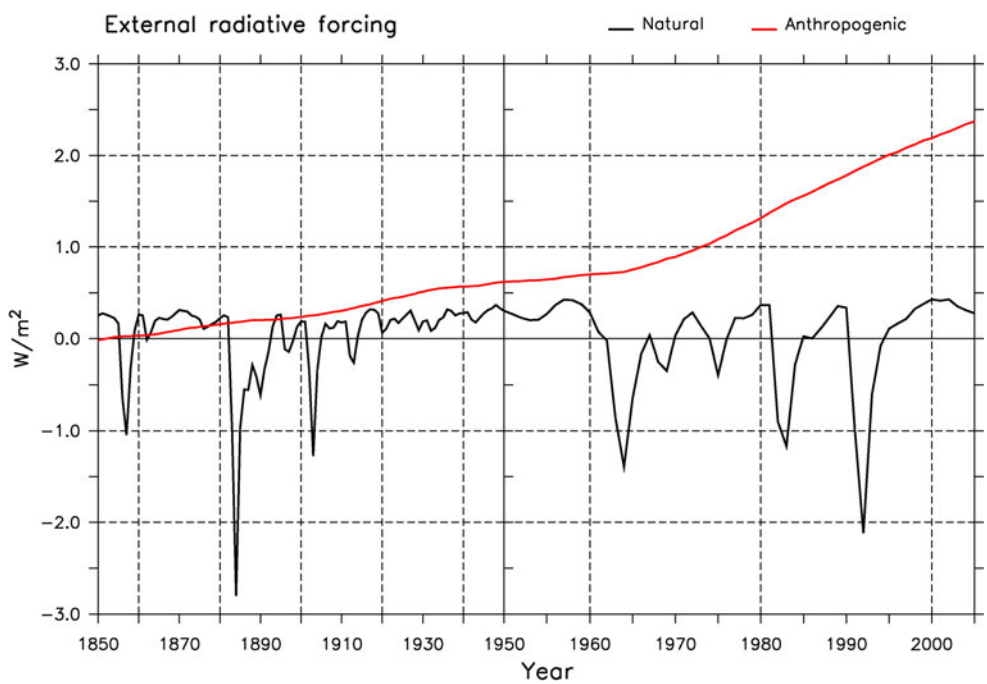

Fig. 1 External forcing used in most of the simulations analysed in this study. Natural forcing corresponds to volcanic eruptions and solar variability. We notice the 3 main eruptions for the last 50 years with Mount Agung (1963), El Chichon (1982) and Pinatubo (1991), which forcing largely dominates over solar. We also notice earlier the impact of two very large eruptions: Krakatoa (1883) and Santa Maria (1904). The anthropogenic forcing includes the increase in greenhouse gases as well as stratospheric ozone and anthropogenic aerosols including direct and indirect effect

Frankignoul and Kestenare 2002). In an attempt to enforce even more the observed SST into climate model, other studies have used a much shorter relaxation timescale (or higher value for γ). For instance Keenlyside et al. (2008) used 4 days up to 30° of latitude (ramping down to no nudging at 60° of latitude), which is 15 times stronger than restoring used in this study. Similarly, Dunstone and Smith (2010) used a restoring coefficient γ 15 times stronger, Pohlmann et al. (2009) 6 times stronger and Luo et al. (2005) 60 times stronger than the one used here. Furthermore, contrary to Keenlyside et al. (2008), we include the high latitudes but, to avoid spurious interactions, we do not apply nudging in the model at grid points where the sea-ice cover is larger than 50 %. In contrast to several other studies, we deliberately choose not to include any nudging below the ocean surface essentially to avoid tampering with ocean internal dynamics, which contain the predictive signals. The assumption is that on sufficiently long time scales, the ocean circulation is able to propagate surface signals into the ocean interior, similarly to a forced oceanic run and as in the real ocean. This strategy of course relies on the quality of the ocean GCM and the ability of the coupled model to reproduce the observed modes of variability. It also probably depends on the length of the period during which the nudging is applied. We do not apply any salinity restoring, mainly due to the unavailability of products with a sufficient time and space coverage.

Finally, a set of three-member ensembles (called hindcasts in the following) are launched on the 1st January 1961 and every 5 years afterwards from one member of the nudged ensemble. They use the same external forcing as the historical (and the nudged) simulations and no restoring at all. These simulations follow a RCP4.5 scenario for the years beyond 2006. The initial conditions for the different members are very simply obtained by perturbing the SST from the nudged simulation with an anomaly that has been chosen randomly for each grid points in the interval [−0.05, 0.05 °C] (with an equiprobable distribution for each value over this interval) mimicking a non-Gaussian white noise perturbation. No perturbation has been applied for the grid points under sea-ice cover. The duration of the different three-member ensembles is 10 years. These hindcasts follow the CMIP5 protocol (Taylor et al. 2012) and are available in the CMIP5 database.

The 20-year internal variability cycle, found in the subpolar basin in the IPSL–CM5A–LR 1,000-year control simulation, is challenging to validate due to the combined effect of natural and anthropogenic radiative perturbation and the short available observational record. Nevertheless, as a first step, we show in Fig. 2 that in the Nordic Seas the winter SST from HadISST (Rayner et al. 2003) exhibits a significant frequency peak of variability at around 20 years as in the model. A 20-year peak was also found for a longer time period in Greenlandic cores (Chylek et al. 2011) and in an oceanic core north of Iceland (Sicre et al. 2008) reconstructing SSTs over the last 2,000 years. These results therefore strongly suggest the existence of such a 20-year cycle in the real ocean. The fact that the present model also exhibits this 20-year cycle even though there are large biases in its simulation of the North Atlantic oceanic characteristics can be fortuitous. We nevertheless take advantage of this property to further examine the possible existence of the 20-year cycle in the real world and its role for the AMOC synchronisation between reconstructions and the historical and nudged simulations.

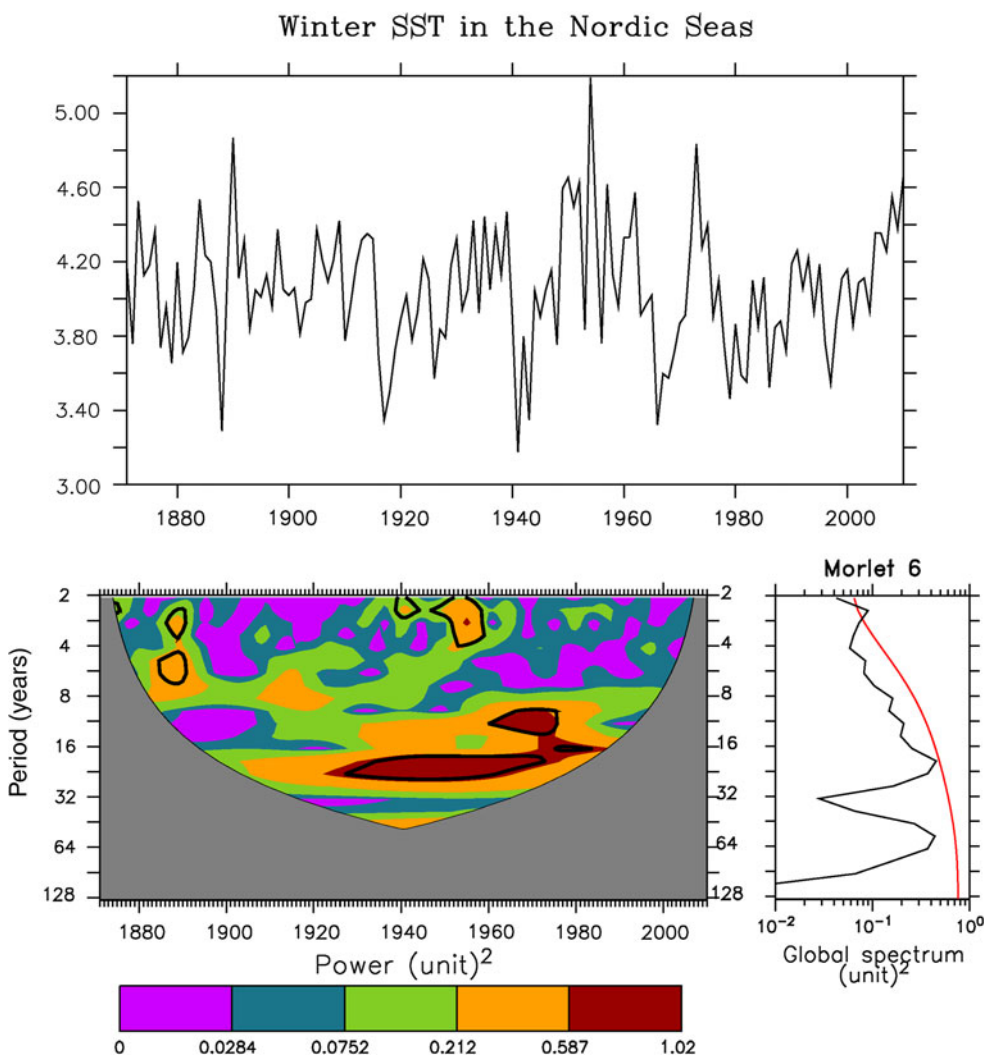

Fig. 2 *Top* time series of SST averaged over a Nordic Seas *box* (0°–20°E, 66°N–78°N) in winter (December–February) from HadISST (Rayner et al. 2003). *Bottom left* wavelet analysis of the signal. The region significant at the 95 % level are marked using *bold contours*. *Bottom right* power spectrum of the signal in *black* compared to an AR1 signal (in *red*)

3 Initialising the AMOC with SST nudging

3.1 Oceanic heat content variations

Figure 3a shows that, on the global scale, the heat content in the first 700 m of the ocean increases in the nudged and historical simulations, with a similar amplitude compared to the observation-based estimates from Levitus et al. (2009). For the period 1955–2005 a linear regression has a coefficient of 69.5 TW in the data, 54.9 TW in the nudged simulations and of 75.2 TW in the historical simulations. The relatively strong climate sensitivity of the IPSL–CM5A model, described by Dufresne et al. (submitted), is thus also illustrated here. We also note possible signatures of the largest volcanic eruptions with a slight decrease in the global heat content following Mount Agung (1963), El Chichon (1982) and Pinatubo (1991) eruptions both in the observations and simulations (Fig. 3a).

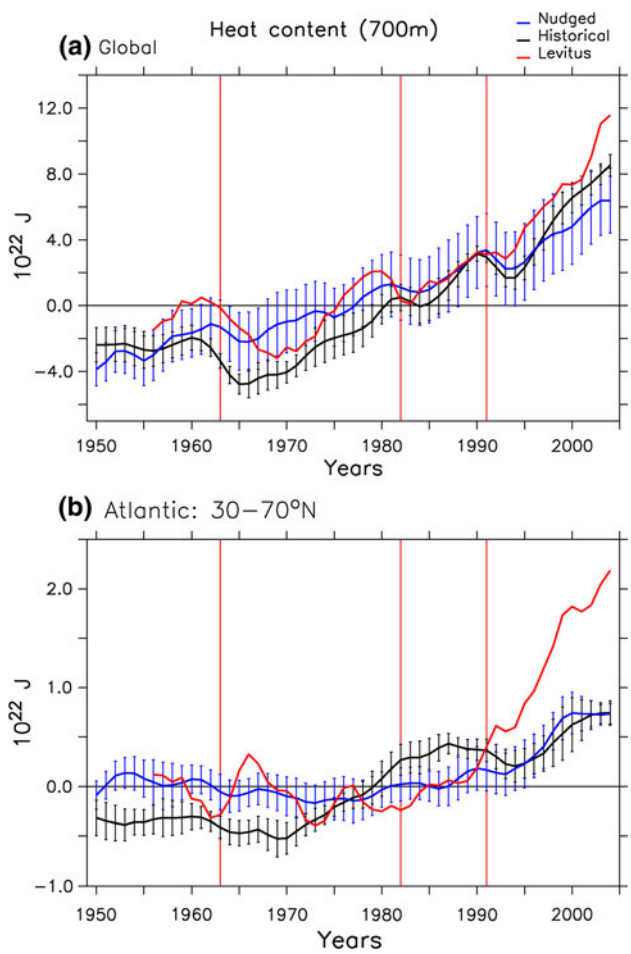

Fig. 3 Heat content from Levitus et al. (2009) with slight recent improvements in *red* (cf. http://www.nodc.noaa.gov/OC5/3M_HEAT_CONTENT), from the nudged simulations in *blue* and from historical simulations in *black* expressed in 10^{22} J. **a** for the global ocean, **b** over 30°–70°N in the Atlantic. The reference period is 1961–1990 and a 3-year running mean has been applied to all the data. The *error bar* for historical and nudged simulations corresponds to two standard deviations computed for each five-member ensemble. The *red vertical lines* represent the years with a large eruption i.e. the Mount Agung in 1963, EL Chichon in 1982 and Pinatubo in 1991

When focusing on the North Atlantic (30–70°N, Fig. 3b), the cold bias in the historical simulations for the beginning of the period is more evident, as well as the fact that this bias is partly corrected by the nudging. There is also more variability in the data as compared to the global average, which is not well reproduced even in the nudged simulations. The observations lie in the uncertainty range of the nudged simulations for the period 1955–1990. The rapid heat content increase observed from the 1990s is somewhat present in the simulations but is too weak in both the historical and nudged simulations.

These results differ the ones found in Keenlyside et al. (2008), where changes in heat content in the North Atlantic was decreasing for the last 50 years (Pohlmann, personal communication), contrarily to in situ data from Levitus et al. (2009). As described earlier, the present experimental design is similar to that of Keenlyside et al. (2008) in that it does not include any oceanic subsurface information. Nevertheless, we do not find such a misrepresentation of the heat content changes for the last 50 years. We therefore conclude that the misrepresentation of the oceanic heat content changes found in Keenlyside et al. (2008) was not necessarily only due to the absence of deep oceanic information (Dunstone and Smith 2010), but also likely to their very strong surface SST restoring, which may have led to non-physical heat fluxes and hence heat uptake. These results give confidence in the opportunity to impose a weaker restoring constraint.

3.2 Initialisation of the AMOC

The reconstruction of the AMOC at 48°N by Huck et al. (2008) and the AMOC index from Latif et al. (2004) are shown in Fig. 4a. Although they are fully independent, these two reconstructions show strong similarities, particularly in the 4 Sv decrease from 1960 to 1975 and the two local maxima around 1980 and in the mid-1990s. The historical ensemble simulations also show two local maxima, around 1977 and 1998 (Fig. 4c). In the nudged ensemble, the maxima occur similarly around 1978 and 1997 (Fig. 4b). On the other hand, for the period before 1975, both the historical and the nudged ensemble means are very different from the reconstructions. When computing a correlation with Huck et al. (2008) reconstruction using a 20-year moving window, we find significant correlation at the 90 % level (accounting for the serial autocorrelation following Bretherton et al. 1992) from year 1977 with correlation of 0.77 for the nudged ensemble mean and no significant correlation for the historical

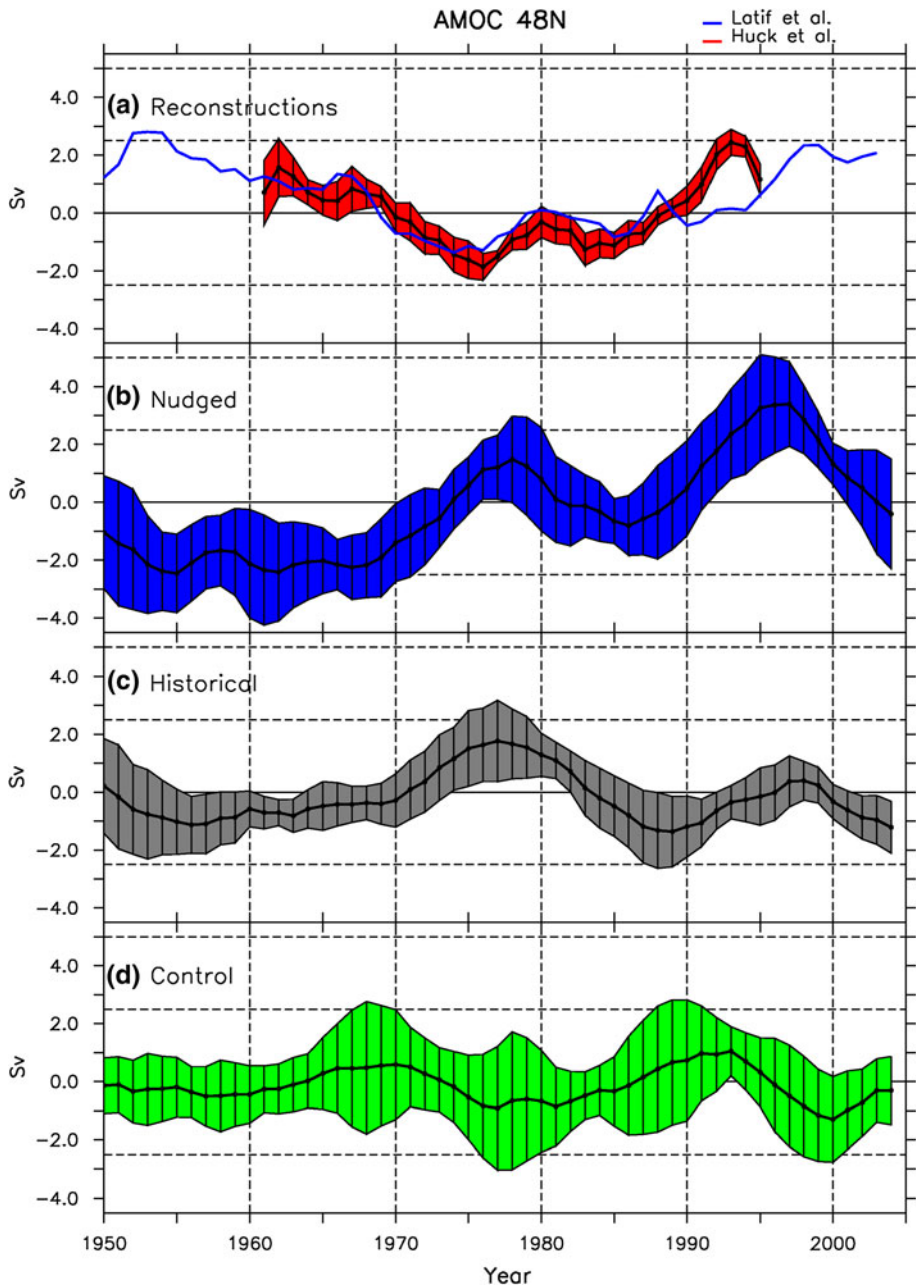

Fig. 4 AMOC indices defined as the maximum of the meridional overturning stream function in the Atlantic at 48°N. **a** Reconstructions from Huck et al. (2008) in *red* and Latif et al. (2004) in *blue*, **b** mean and standard deviation (STD) of five-member ensemble of nudged simulations over the period 1948–2005, **c** mean and STD of historical simulations without any initialisation method, **d** mean and STD of control simulations without any initialisation and external forcing. A 3-year running mean has been applied to all the data

ensemble mean (not shown). This suggests that the SST nudging has had a significant impact to initialise the AMOC at 48°N. In contrast and as expected, the control simulation does not show any clear relationship with the reconstructions (Fig. 4d), illustrating the fact that the skill found in the nudged and historical simulations is not related to the initial conditions. Both the historical and the nudged simulations therefore show some ability for AMOC synchronisation with the reconstruction. The phase agreement in low frequency variability of the AMOC is present in the historical simulations, but not sufficiently to yield significant correlation. It is improved in the nudged simulations, in particular in terms of amplitude, which may explain the significant correlation found from 1977 onward.

In order to understand the processes explaining the two local maxima in the AMOC for the period 1970–2005 in the historical and nudged simulations, we analyse the variations of the winter mixed layer depth in the main convection sites driving the AMOC in the North Atlantic. The sites are located in the Nordic Seas, south of Greenland just outside the Labrador Sea, and in an extended area south of Iceland including the Irminger Sea (Escudier et al. submitted). Variations in the mixed layer depth and in surface density in the sites south of Iceland are significantly correlated with the AMOC variations in the 1,000-year

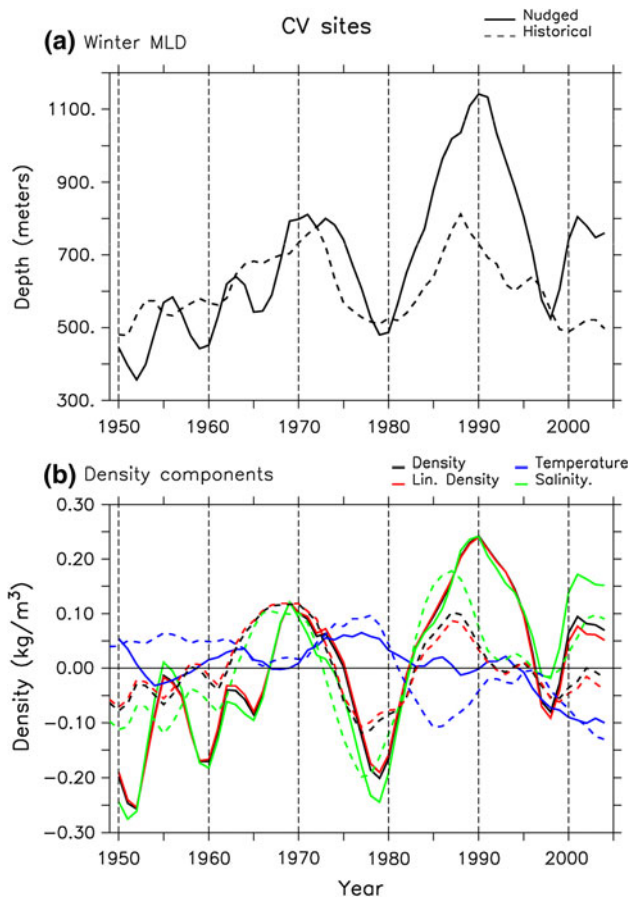

Fig. 5 Time series of the 5-members ensemble mean for the nudged simulations (*continuous line*) and historical simulations (*dashed line*). **a** Winter mixed layer depth averaged over the convection sites located south of Iceland, which are the main driver of AMOC variability in this model (see Fig. 2 from Escudier et al. for the exact definition of this region), **b** surface density (in *black*) averaged over the same region, with its linear decomposition into haline (*green*) and thermal (*blue*) component as well as the sum of the two (*red*) representing the linearized density. A 3-year running mean has been applied to all the data

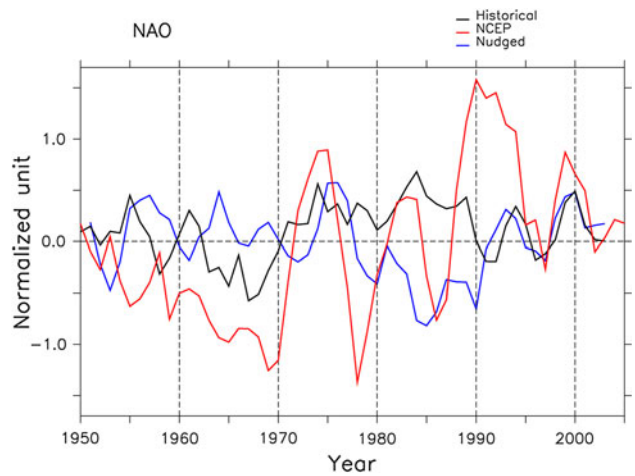

Fig. 6 NAO index computed as the principal component of the first Empirical Orthogonal Function of SLP over the North Atlantic (30°W–80°E, 20°N–80°N) in NCEP data (Kistler et al. 2001, *red curve*), ensemble mean of the historical simulations (*black*) and ensemble mean of the nudged simulations (*blue*). A 3-year running mean has been applied to all the data

control simulation under preindustrial conditions with a time lag of 5–10 years (Escudier et al. submitted). Consistently and as seen in Fig. 5a, there are two local maxima for the mixed layer depth averaged over the convective areas in 1973 and 1988 in the historical simulations and in 1971 and 1990 in the nudged simulations. Deep mixed layers in the convective areas are in phase with local anomalously strong surface densities (the correlation between the two time series is indeed 0.92 in the nudged simulations and 0.81 in the historical ones). We decompose this surface density into its haline and thermal components using a linear decomposition (Fig. 5b). The linearized density is practically the same as the non-linear one (Fig. 5b, $r > 0.99$) thereby validating the linear assumption. In agreement with findings in the control simulation (Escudier et al. submitted) and other climate simulations (e.g. Delworth et al. 1993; Mignot and Frankignoul 2005; Msadek and Frankignoul 2009), the haline component drives the main density variations in both the nudged and historical simulations, while the thermal component is smaller in magnitude. In the historical simulations, it is furthermore most of the time in opposite phase with the density variations. In free fully coupled conditions (control and historical simulations), it is therefore the increase in SSS in the convection sites that triggers the convective events, while the SST increase during most of these episodes acts to damp the convective activity.

Nevertheless, Fig. 5b also shows that in the nudged simulations, there is more to the SST behaviour: around 1985 in particular there is a positive thermal contribution to the density in the nudged simulation, while the density anomalies are also positive (same sign as the haline contribution). In this case, SST anomalies add to SSS anomalies to further enhance the positive density anomaly leading to the subsequent convective event. The latter is consequently much larger than in the historical ensemble. The SST nudging in the convection sites could partly explain this feature and therefore the enhanced amplitude of the convection in the 1980s and finally better skill in reproducing AMOC variations as compared to the reconstructions in the 1990s (Fig. 4). The 1980s correspond to a period of persistently high NAO index (Hurrell 1995, Fig. 6), which led to persistent negative heat flux and SST anomalies over the subpolar basin (e.g. Eden and Jung 2001). This induces a persistent negative SST restoring at that time in the nudged simulations (as seen in Fig. 7c), which explains the positive thermal contribution to the

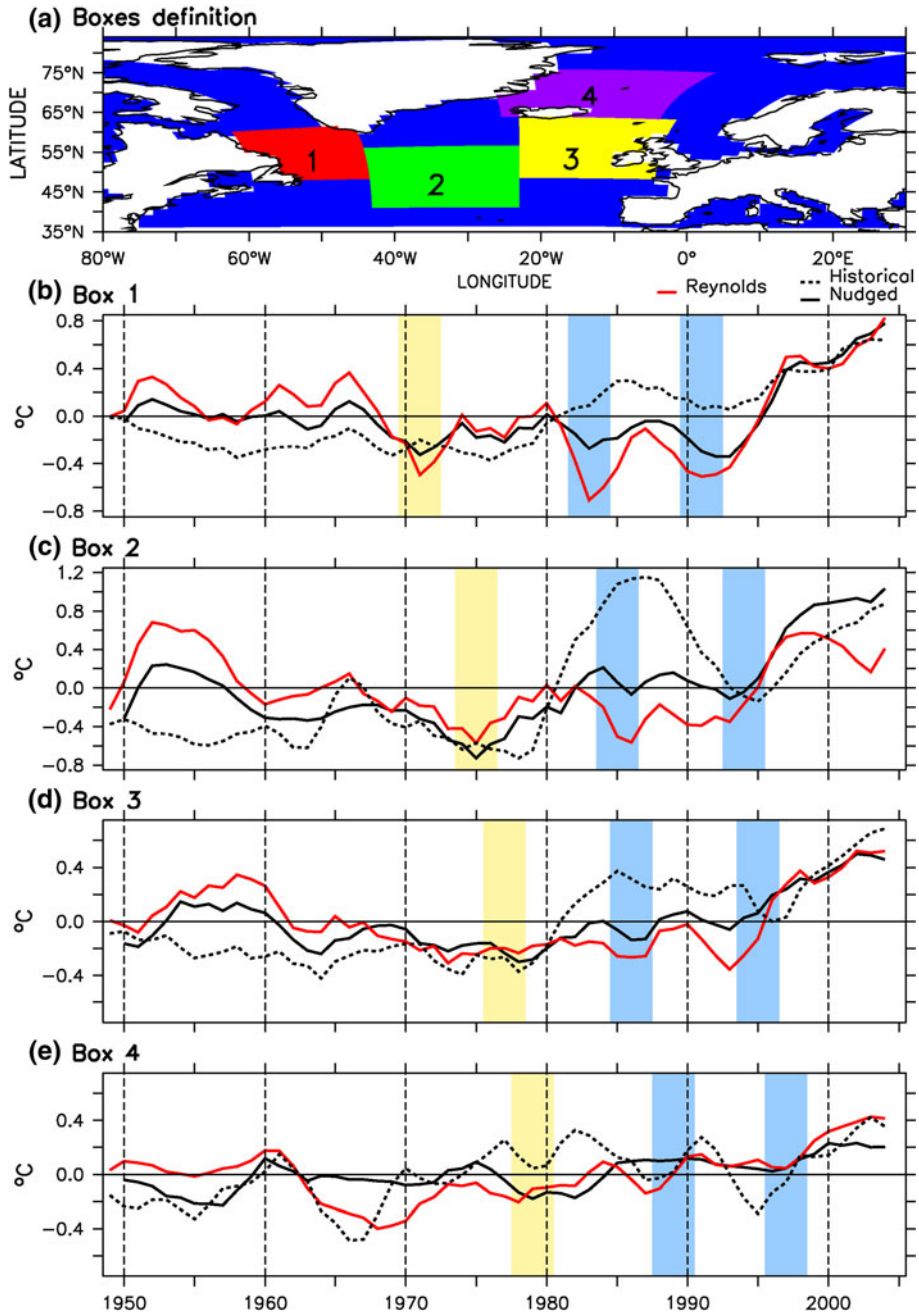

Fig. 7 *Map* and time series illustrating the propagations of SST anomalies in the North Atlantic following the mechanism of GSAs. **a** *Map* of the different *boxes* used for averaging the SST in the following *panels*. **b** Time series of SST averaged over the *box* 1. In *red* are the Reynolds et al. (2007) data and in *black* the mean of the 5-members nudged simulations (*continuous line*) and the historical simulations (*dashed lines*). The time series are centred over the period 1949–2005. **c** Same as **b** but for *box* 2. **d** Same as **b** but for *box* 3. **e** Same as **b** but for *box* 4. A 3-year running mean has been applied to all the data. The *yellow* and *blue* overlaps correspond to propagative events, corresponding to GSAs events

density in the nudged simulations in contrast to the historical simulations (Fig. 5). In summary, the maximum of convection and density anomaly in the late 1980s found both in the nudged and historical simulations is larger than in the nudged because of the positive thermal contribution to density, while it is negative in the historical at that time. Nevertheless, the haline contribution remains the primary contributor to the convective activity both in the historical and nudged simulations, in particular to its timing. We now investigate the origin of the mechanisms involved in these SSS variations.

Figure 8 shows the time series of different indices representing the processes involved in the 20-year cycle found in the control run of IPSL–CM5A–LR (Escudier et al. submitted) for the nudging and historical ensemble means. We begin with the SST in the Nordic Seas, since the SST is the component that is directly affected by the nudging. A signal of negative SST and positive sea-ice cover anomalies is detected for the period 1963–1967 in the Nordics Seas in the historical simulations, as well as in the nudged simulations and Reynolds et al. (2007) data (Fig. 8b, c). To explain this unexpected SST agreement between

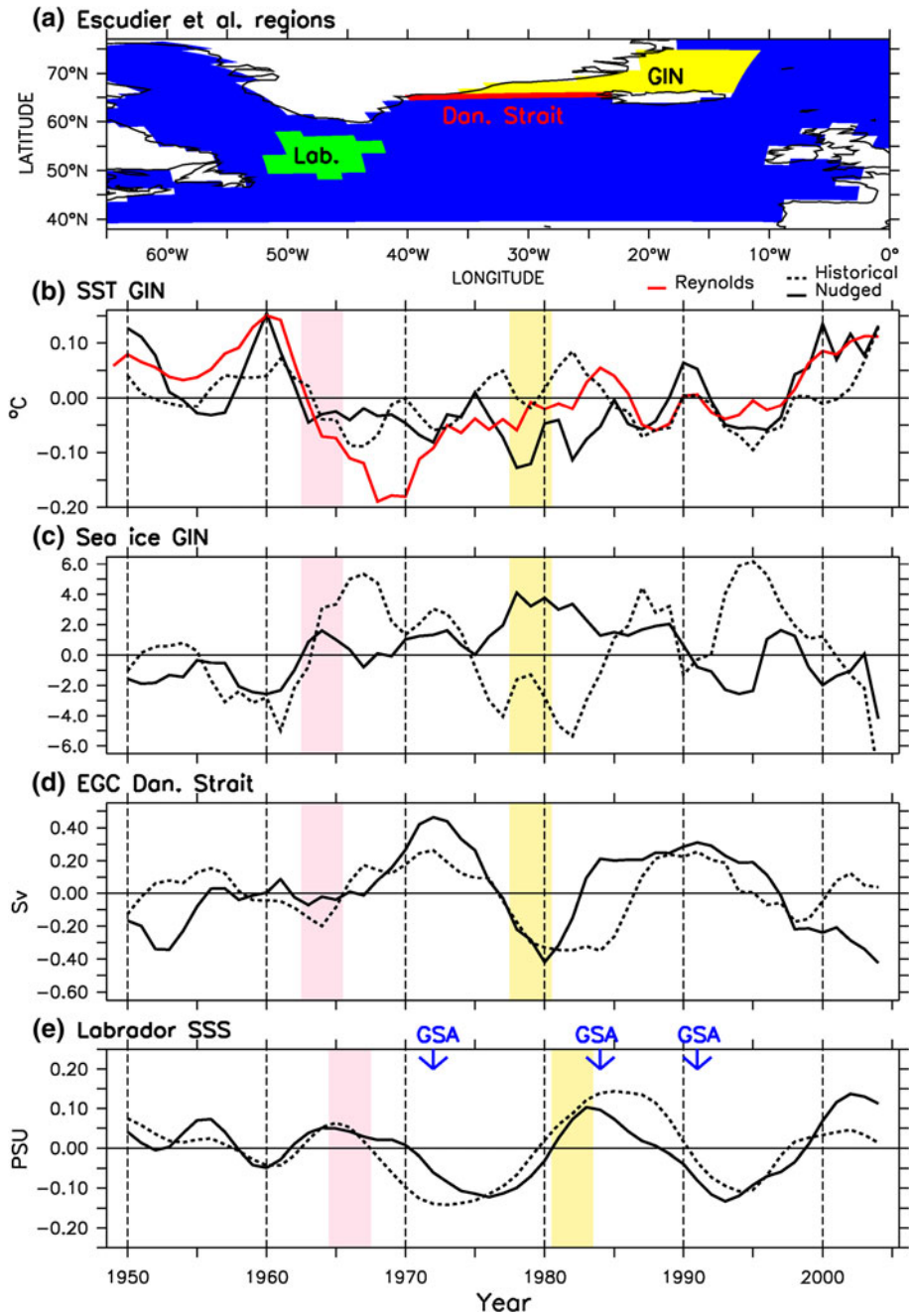

Fig. 8 Time series of the 5-members ensemble mean of the nudged (*continuous line*) and historical (*dashed line*) simulations of different regions represented in **a**. **b** Winter SST in a region in the middle of the Greenland Iceland Norway (GIN) Seas (Reynolds et al. (2007) in *red*, **c** winter sea-ice cover in the GIN Seas, **d** annual mean of East Greenland Current intensity through the Denmark Strait (water with lower salinity than 34 PSU, positive when southward), **e** SSS in the Labrador Sea. A 3-year running mean has been applied to all the data. The *yellow* and *pink* overlaps corresponds to crucial periods commented in the text. The *arrows* with "GSA" correspond approximately to observed GSA following literature (Belkin et al. 1998; Belkin 2004)

observations and the historical simulations, we invoke the negative external forcing related to low solar activities and several volcanic eruptions, including the large Mount Agung event (Booth et al. 1963). The conjunction of these forcings has cooled the Nordics Seas in the simulations in the mid-1960s (Fig. 8b) thereby favouring an increase in sea-ice cover. This increase in sea-ice there diminishes the momentum forcing of the ocean through the wind stress along the Greenlandic eastern coast and thus induces a weakening of the EGC (Fig. 8d), leading to the anomalous accumulation of SSS in the Labrador Sea around year 1968 (Fig. 8e) in both the nudged and historical simulations. Moreover, as shown by Escudier et al. (submitted), the anomalies of sea-ice cover in the Nordic Seas can lead to a local anomalous cyclonic atmospheric circulation in the model and reduce the northeasterly winds along the eastern coast of Greenland. This is also consistent with a weakening of the EGC and thus an accumulation of SSS in the Labrador Sea around year 1968. Nevertheless this effect is not consistently detected both in the simulations and the NCEP reanalysis for the period 1963–1965 (not shown). In any case, this positive SSS anomaly then circulates along the subpolar gyre and affects the convection sites in the early 1970s (Fig. 5), which enhances the AMOC around 1978

(Fig. 4). No consistent link between the SSS anomalies in the Labrador Sea and changes in the subpolar or subtropical gyres intensity has been found both in the nudged and historical simulations (not shown) so that we argue that these SSS anomalies mainly come from the Nordic Seas through the EGC connection.

For the 1997 AMOC maximum in both the nudged and historical simulations, we observe a weakened EGC around 1980 and anomalous positive SSS in the Labrador Sea around 1982 (Fig. 8e), convective events in the late 1980s (Fig. 5) and an increase in the AMOC around 1997 (Fig. 4). We therefore argue that the 20-year cycle mechanism found in Escudier et al. (submitted) is playing a role for the AMOC variations in the historical and nudged simulations and is correctly initialised from the late 1970s thanks to the cooling in the Nordic Seas related to the Mount Agung volcanic eruption starting about 15 years before. Nevertheless we put the stress on the fact that the ocean–sea ice–atmosphere interaction found in the control simulation of the same model by Escudier et al. (submitted) is not clear in these simulations as well as in the NCEP data, leaving room for another processes linking the Nordic Seas and the Labrador Sea. The sea ice insulation effect limiting the atmosphere forcing on the ocean in terms of momentum through the wind stress is a plausible candidate.

To further support this hypothesis of an initialisation of the 20-year cycle by the Mount Agung eruption, which occurs after 60 years without any large eruption (Fig. 1), we take advantage of additional simulations using only natural or anthropogenic forcing (Table 1). Figure 9 shows that the AMOC in the natural ensemble is noisy, but it also exhibits two local maxima around 1978 and 1997, while it is not the case for the anthropogenic ensemble. This clearly strengthens the hypothesis of an initialisation of the subpolar 20-year cycle of the model by the 1963 Mount Agung eruption. The following large eruption (El Chichon) occurs around 19 years, which may hardly modify the phase of the 20-year cycle. Concerning the Pinatubo eruption of 1991, its effect on the AMOC may be found around year 2006, which is beyond the length of the historical and nudged simulations. Its effect on oceanic convection will be discussed below.

3.3 The role of temperature and salinity advection

The east to west propagation of SST anomalies along the subpolar gyre can be seen in the nudged simulations via the restoring term, which is derived from the departure to the Reynolds et al. (2007) observations (Fig. 7). For instance, a negative SST anomaly developed around 1972 in the Labrador Sea in the Reynolds et al. (2007) data and reached the Nordic Seas in 1979 (Fig. 7). The time scale of around 7 years found in the Escudier et al. (submitted) analysis is compatible with such an advection in the observations.

In IPSL–CM5A–LR, the propagation of SST anomalies along the subpolar gyre can be related to a propagation of SSS anomalies of the same sign. We suspect that such association of SSS and SST anomalies is also occurring in the observations, suggesting similar propagation as found for SSS anomalies during Great Salinity Anomaly (GSA) events (Sundby and Drinkwater 2007). The mid 1970s negative SST, and probably SSS, anomaly propagation found in the Reynolds et al. (2007) data can actually be related to the 1970s GSA (Belkin et al. 1998). Moreover we can find other SST propagative events in Fig. 7, which may also correspond to the 1980s and 1990s GSAs. Thus, we also find clues in the real ocean of the association of negative SST anomalies with negative SSS anomalies initiated in the Labrador and then propagating along the subpolar gyre. The GSA in the 1980s has been related to NAO forcing (Belkin 2004) and not directly to Arctic connection through the Fram and Denmark straits. This 1980s GSA is actually not seen in the historical simulations and hardly seen in the nudged simulations (Fig. 8e). In the model, the SSS minima in the subpolar gyre (that we associate to the observed GSAs) explain AMOC minima (as in Häkkinen 1999). Thus we argue that for instance the GSA found in the Labrador Sea around 1972 may have limited the convection around 1977 leading to an AMOC minimum for the period 1982–1987, which is consistent with the AMOC reconstructions (Fig. 4). These results confirm the plausibility of the time scale found in this model for the advection of anomalous SST and SSS along the subpolar gyre and Nordic Seas as well as the occurrence of such advective events in the real world.

To summarize, we argue that the occurrence of an AMOC maximum around 1978 is related to the external forcing, in particular the 1963 Mount Agung volcanic eruption. This external event resets and synchronizes the 20-year AMOC cycle, which then further explains a local maximum around 1997 both in the historical and the nudged simulations. The nudged simulations better capture the amplitude of this maximum as compared to reconstructions, because it includes the impact of an exceptionally persistent positive NAO on the subpolar SST in the late 1980s and beginning of the 1990s in contrast to the historical simulations where the NAO is not correctly phased. We also note that the model reproduces the 1970s and 1990s GSAs, while the 1980s GSA is mostly missed.

4 Potential predictability of the AMOC over the last 50 years

Persechino et al. (submitted) found potential predictability for the AMOC 5–10 years ahead in a perfect model study using the present model. Since we have shown some degree

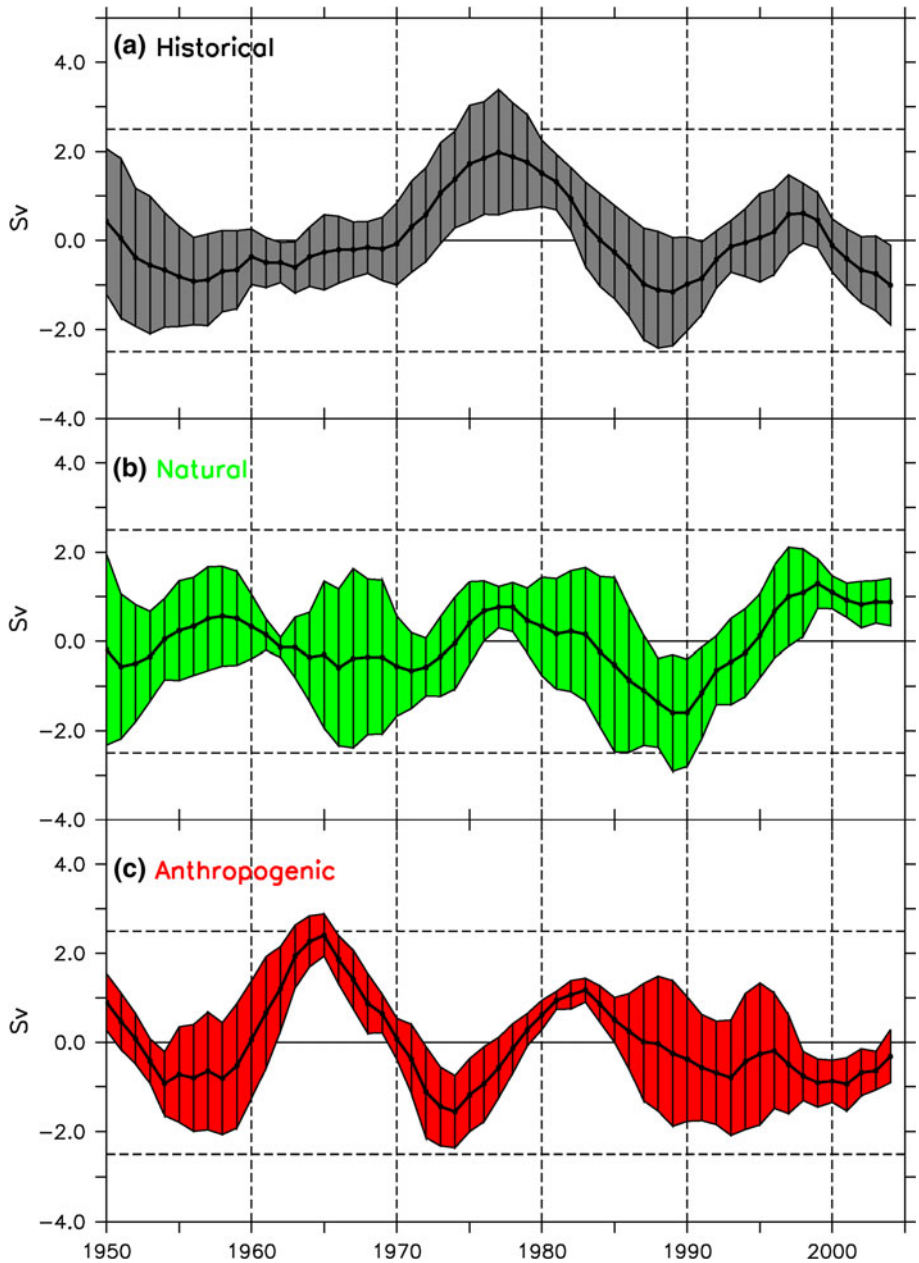

Fig. 9 Same as Fig. 4 but for **a** the historical simulations, **b** the naturals simulations and **c** the anthropogenic simulations (cf. Table 1)

of synchronisation between the nudged ensemble and the AMOC reconstructions, the hindcast simulations starting from one of the nudged simulations may provide predictive skill. Note that as indicated in Sect. 2 and due to computing time limitations, these ensembles of three hindcasts are only launched from one member out of the five nudged simulations. The AMOC of the selected initialised simulation is shown in Fig. 10 (black curve) and even though it differs slightly from the ensemble mean analysed before, it also presents two local maxima after 1970, namely around 1985 and 1995. The hindcasts (colour curves in Fig. 10) capture the AMOC variations of the nudged simulation over the period 1960–1980, with an increase in the 1960s and a decrease in the 1970s. However, the AMOC increase in the 1980s and 1990s is not reproduced. On the other hand, the decrease at the end of the 1990s is relatively well predicted. An AMOC stabilisation in the years 2000 is seen in Fig. 10 (especially in the hindcasts starting in 2006). The reconstructions used here do not extend beyond 2005 so we cannot evaluate this stabilization against observations. Data from Kanzow et al. (2010) nevertheless indicates a stable AMOC for the period 2004–2008 in agreement with what is found here. To explain this stabilisation, we note in Fig. 5 a maximum of MLD related to SSS in the early 2000s both in the historical and nudged simulation, occurring only 10 years after the previous one around

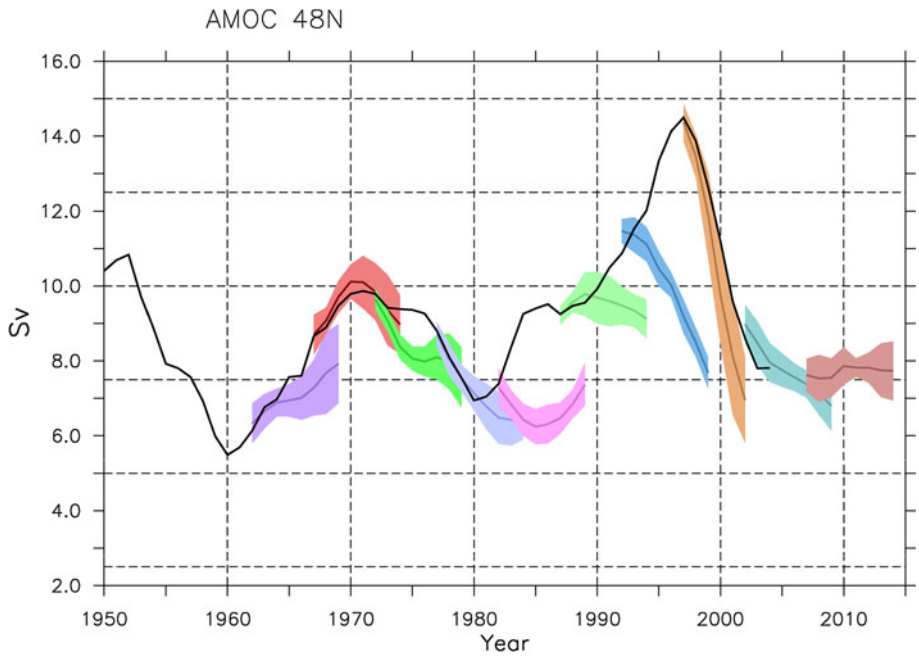

Fig. 10 AMOC maximum at 48°N in a nudged simulation (*black line*) and for different 3-members ensemble of 10 years launched every 5 years. The *coloured lines* stand for the ensemble mean while the overlaps represent two STD of each ensemble. A 3-year running mean has been applied to all the time series

1990. This is at odds with the 20-year cycle mechanism, which should have led to a maximum around 10 years later. We propose that this behaviour is related to the Pinatubo eruption occurring 10 years before, which may have partially reset the 20-year cycle leading to a stabilisation instead of the expected minimum, similarly to a destructive interference.

In order to quantify the skill of the hindcasts in capturing the AMOC evolution of the nudged simulation, as a first statistical step, we compute correlation coefficient of 10-year mean as a measure of skill of predictability (Keenlyside et al. 2008) both for the AMOC indices at 48°N (Fig. 11a) and for the maximum taken between 10 and 60°N and below 500 m (latitudinal maximum, Fig. 11b). We evaluate the correlation of the time series composed by the 10-year average for the hindcasts and the series of the associated 10-year average in the nudged simulation (we call this averaging period the "lead-time average" in the following, which is here of 10 years). In spite of the weak prediction of the AMOC evolution in the 1980s and 1990s, the correlation between the AMOC indices in the hindcasts and in the nudged simulation is very high (>0.8) and significant at the 95 % level. For both indices, it is much higher than the correlation with the persistence time series (constructed assuming a persistence of the AMOC value the year before the launch of the hindcasts with a damping term following Pohlmann et al. 2004). Moreover, we find that the heat transport at 20°N in the Atlantic in the hindcasts and the nudged simulation are correlated at 0.97, which again beats the persistence (Fig. 11c). We compare this skill to the lack of skill in forecasting the heat transport at 20°N in the Pacific Ocean (Fig. 11d). This highlights that in this model the potential for predictability related to oceanic heat transport is stronger in the Atlantic Ocean than in the Pacific. We attribute this result to the potential predictability of the AMOC (Persechino et al. submitted) and its dominant role in the meridional heat transport in the Atlantic (as shown by Escudier et al. submitted) in this model, and potentially in the real world. In the North Pacific there is no deep convection and neither a large-scale MOC cell and therefore no such relationship.

A slight drift is seen in most indices in Fig. 11. For the AMOC, this could be related to the absence of SSS initialisation or to the extreme NAO observed in the 1980s–1990s, which could both lead to large convective events. Nevertheless, detrending the fields in Fig. 11 does not modify the main results found here and only slightly affects the correlations.

In order to further evaluate the AMOC hindcasts with respect to observations, we compute the correlation skill score with the AMOC reconstruction at 48°N from Huck et al. (2008). All time series are considered with a 10-year lead-time average as above. We start the time series in 1966 in order to avoid the earlier time period during which the model had not enough time to be correctly initialised. The nudged simulations as well as the hindcasts launched from this simulation from 1966 onwards are significantly correlated with the "observed" AMOC (Fig. 12). In contrast, neither the corresponding historical simulations nor the persistence have any significant correlation with the reconstruction. This diagnostic confirms that we have successfully initialised the AMOC, which eventually provides increased predictability for this index in the hindcasts as compared to simulations using only external forcings

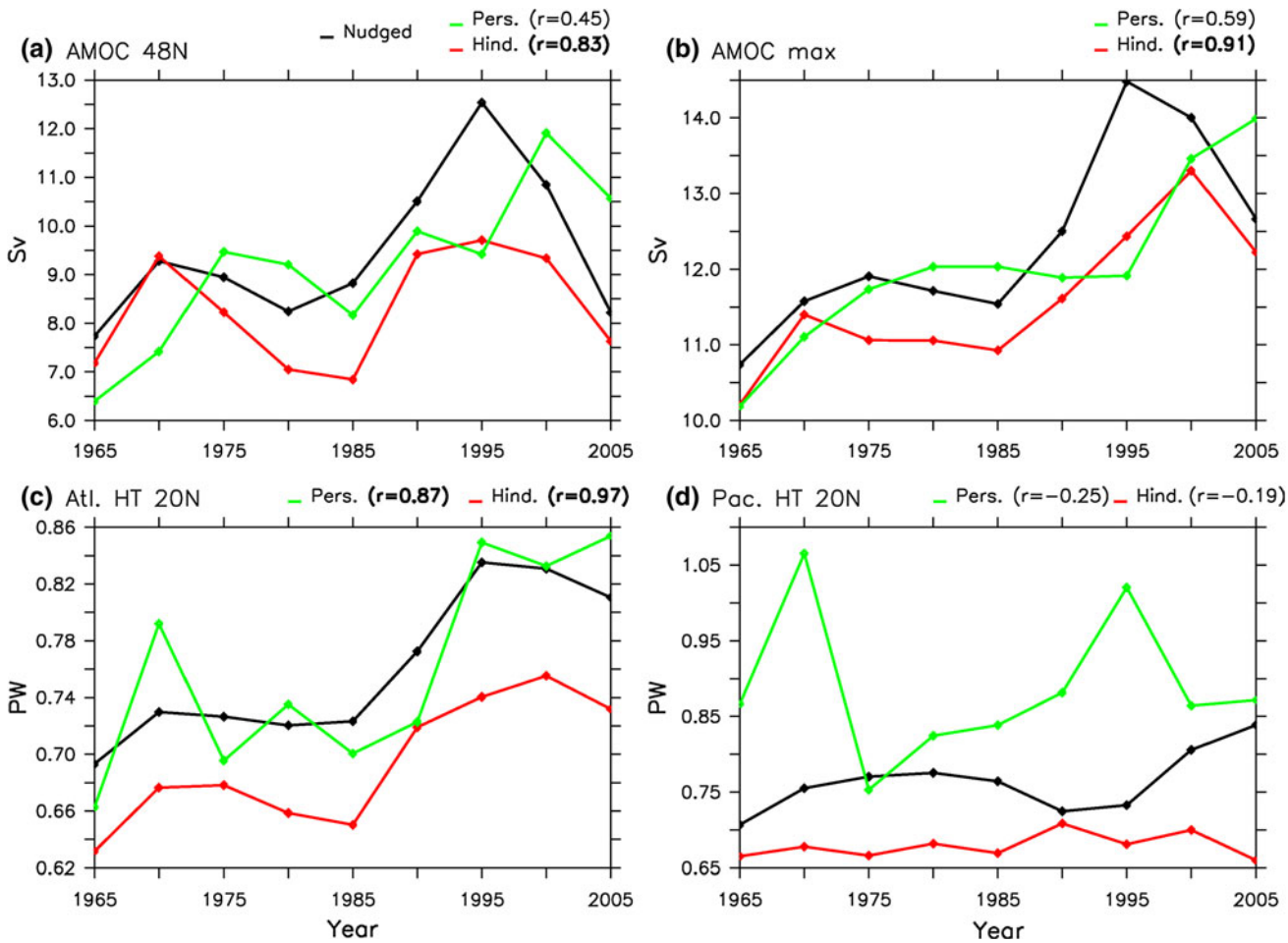

Fig. 11 Correlation skill score: each point corresponds to the 10-year mean made around the date of the point. In *black* is the nudged simulation; in *red* the ensemble mean of the 10-year free ensemble (Hind.) and in *green* is the persistence (Pers.) following Pohlmann et al. (2004) definition. Note that the damping term was computed using the 1,000-year control simulation. **a** AMOC at 48°N, **b** AMOC maximum, **c** zonal-depth average of Atlantic heat transport at 20°N, **d** zonal-depth average of Pacific heat transport at 20°N. When the correlations with the nudged simulation are signifcant at the 90 % level they appear in *bold*

and no initialisation technique. Other lead-time averages have been tested and show a similar behaviour from 4 years lead-time average (no significant correlation for lower lead-time average, potentially due to the large AMOC inter-annual variability).

In order to evaluate any potential predictability in the global climate, notably associated with the AMOC predictability, we analyse the predictability of two important climatic fields (2-m air temperature and precipitation), using the same correlation skill score but applied at each grid point of the model to produce a correlation map. In order to avoid the general signal related to increased greenhouse gases and associated increase in temperature, as a first step, we regress all the temperature and precipitation fields on the anthropogenic forcing and detrend all the fields using these regressions, following the van Oldenborgh et al. (2012) methodology. Due to the limited observed precipitation records, we take the nudged simulation as the target for all the correlation computations. Figure 13 shows that the temperature exhibits a large ellipse of significant correlation in the North Atlantic encompassing part of Europe and eastern North America. Such a pattern can be seen as an AMOC signature on climate in the model (Persechino et al. submitted), consistently with Knight et al. (2005) and is only faintly seen in the persistence (Fig. 13b) and historical simulation (Fig. 13c). This result thus highlights the potential climatic impact of AMOC initialisation in this model. Note that hints of predictability are also detected over the northern part of the African continent as well as localized areas bordering the Labrador Sea. Investigation of the origin of these predictive skills is left for future studies.

Precipitation generally exhibits lower correlations than temperature and appears therefore less predictive. Nevertheless a pattern of significant correlations between the nudged simulation and the hindcasts can be seen in the

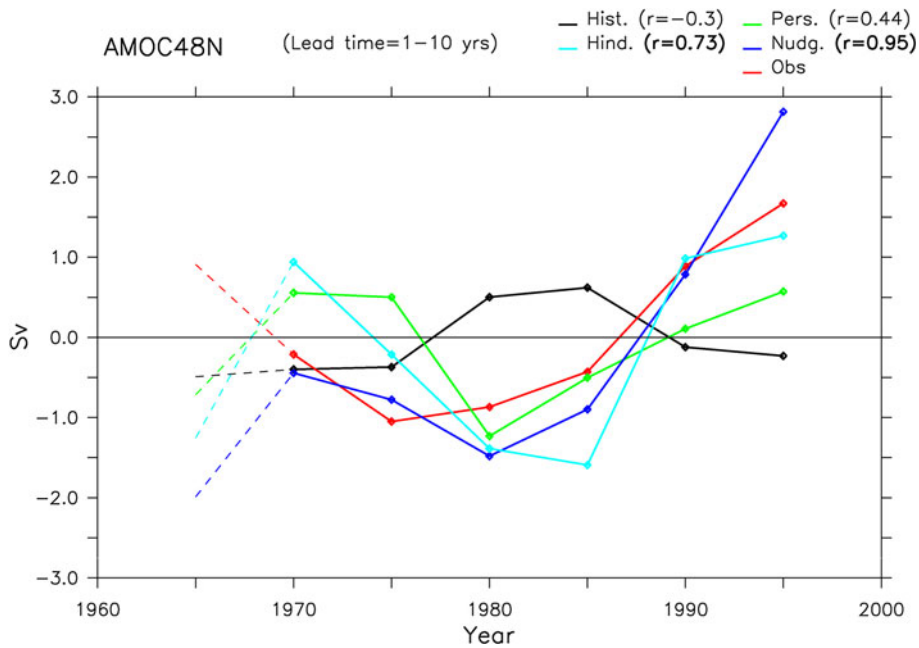

Fig. 12 Same as Fig. 11b but using the reconstruction from Huck et al. (2008) for the AMOC at 48°N as the reference (*red curve*, Obs). The *black curve* stands for the historical simulations (His.), the *green curve* for the persistence (Pers.), the *blue curve* for the nudged simulation (Nudg.) and the *light blue curve* for the hindcasts (Hind.). The correlations have been computed with the reconstruction for the period 1970–1995 (the first decade omitted). When these correlations are significant at the 90 % level they appear in *bold*

Atlantic around 15°N encompassing the Sahelian region, the Caribbean and Central America. Once more, this signature is not present in the persistence and in the historical simulations. Such a fingerprint could also be related to AMOC variations since changes in heat transport and meridional temperature gradient over the Atlantic can affect the inter-tropical convergence zone location, as observed for large weakening of the AMOC in models (Stouffer et al. 2006; Swingedouw et al. 2009), in paleodata (Peterson et al. 2000) or for variations of the Atlantic multidecadal variability (Zhang and Delworth 2006). In the IPSL model, weak potential predictability of precipitation in the northern tropical Atlantic was indeed detected, linked to AMOC variations (Persechino et al. submitted). Here, the correlation remains small, at the limit of the statistical significance, but since precipitation is of key importance in this region, even a low predictability can be of interest.

5 Discussions and conclusions

We have analysed the initialisation of the AMOC from several five-member ensemble simulations using the IPSL–CM5A–LR model as compared to two independent reconstructions of the AMOC for the last 50 years. We have considered both non-initialised historical simulations forced by observed external forcing and initialised simulations using the same external forcing. The initialisation is done via SST anomaly nudging, using a surface SST restoring term based on Reynolds et al. (2007) SST anomalies for the 1949–2005 period and using a feedback coefficient with a physically based amplitude. We chose not to include nudging below the surface to avoid tampering with ocean internal dynamics, which contain the predictive signals.

The historical and nudged ensembles both simulate two reconstructed local AMOC maxima around 1980 and 1995. The timing as well as the amplitude of the nudged ensemble AMOC maxima is in better agreement with the reconstructions, in particular regarding the large AMOC maximum in the 1990s. We explain these results through the triggering of a 20-year internal mode of variability found in the control simulation of the same model, which also appears to be present in the SST from HadISST data in the Nordic Seas for the last 140 years. This triggering, occurring both in the non-initialised and in the initialised simulations, is due to the external forcing and most notably to the Mount Agung volcanic eruption starting in 1963. This eruption leads to a cooling of the Nordic Seas, and a local sea-ice cover increase sufficient to reset the 20-year internal cycle present in this model (Escudier et al. submitted). We propose that the cooling of the Nordic Seas leads to weakening the EGC notably through the insulation effect related to a larger sea-ice cover in winter. This results 3 years later in a large SST and SSS positive anomalies in the Labrador Sea due to the reduction of fresh and cold water coming from the EGC. These anomalies then circulate along the subpolar gyre and increase the convection on their path. This enhances the AMOC around 15 years after the initiation of sea-ice cover anomalies in the Nordic Seas. The better representation of the 1990s AMOC maximum in the nudged simulations as compared to the historical is related to an additional effect of the SST

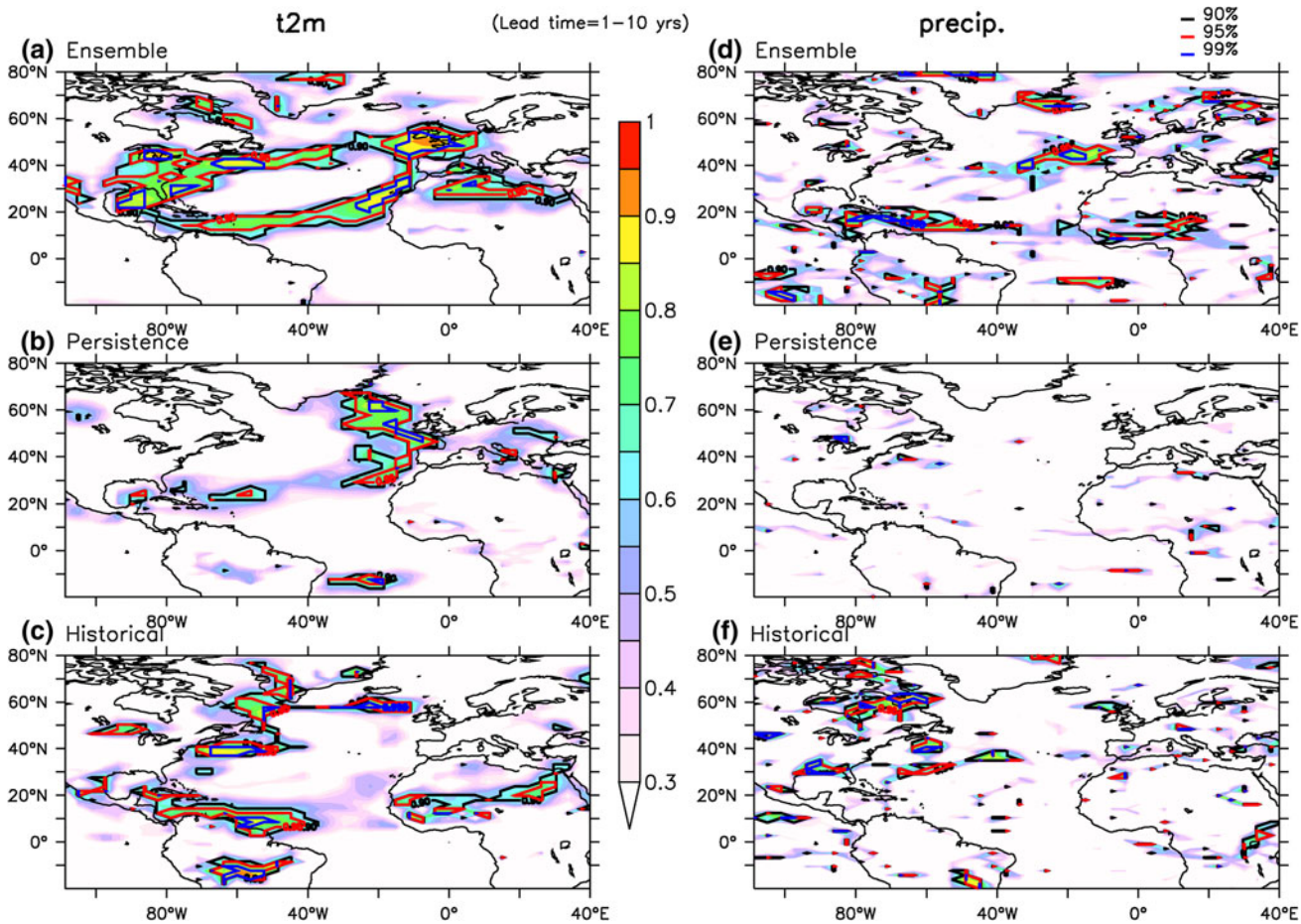

Fig. 13 Correlation skill score (cf. Fig. 11) represented as *map* for the correlation of variables with the nudged simulation for temperature (*left*) and precipitation (*right*). All the fields have been linearly detrended with a regression over the anthropogenic forcing (*red line* from Fig. 1). The first line is the correlation of the nudged 10-year mean simulation with the ensemble, the second for the persistence and the third for the free historical run without any nudging. The significance of the computed correlation have been estimated using a *t* test and the 90 % confidence interval is represented by the *thick black lines*, the 95 % is in *red* and the 99 % in *blue*

restoring over the subpolar gyre in the 1980s. This restoring actually cools the subpolar gyre during several years, due to anomalous positive NAO in the observations, concomitant with a large positive SSS anomalies over the convective sites related to the earlier phasing of the 20-year cycle through the Mount Agung eruption. The nudging thus induces a decoupling between SST and SSS anomalies in the subpolar gyre and allows a constructive effect of the two on the density. In the historical simulations, there is no such exceptional persistent NAO positive phase in the 1980s, which does not cool the subpolar gyre. On the contrary, in these simulations, the subpolar gyre is indeed rather warmer at that time due to the positive SST anomalies, which propagated from the Labrador Sea together with positive SSS anomalies following the 20-year cycle mechanism. In the nudged simulations, the positive SSS anomalies induced by the preceding cycle are associated with negative SST anomalies due to exceptional NAO conditions. These anomalies add up in terms of density and convection, and this explains the large AMOC maximum found in the 1990s in the nudged simulations as well as in reconstructions.

We then analyse a three-member ensemble of hindcast simulations launched every 5 years from one of the nudged simulations. The correlation skill score for the AMOC is statistically significant (90 % level) from 1966 to 2005 with the Huck et al. (2008) reconstruction both for the nudged simulation and the hindcasts, while it is not the case for the historical simulations and the persistence. This skill in AMOC prediction leads to significant correlation skill for 2-m atmospheric temperature in the regions surrounding the North Atlantic as well as a weak signal for precipitation in the Sahelian and Central America regions. Significant skill is also found for the oceanic meridional heat transport in the Atlantic but not in the Pacific. This gives credit to the role of the AMOC for predictability.

No AMOC reconstruction is directly associated with the Reynolds et al. (2007) data set used for nudging the initialised simulation. Thus, in contrast to other studies (Pohlmann et al. 2009; Dunstone and Smith 2010), we do not compare the initialised AMOC with that of the reanalysis used for nudging the initialised simulation. The AMOC reconstructions used for validations in the present study are fully independent of the IPSL–CM5A–LR model and the data used for the initialisation. As a consequence, the agreement we find is particularly striking. The mechanisms we highlight in these experiments confirm the importance of the positive NAO phase for the AMOC maximum in the 1990s as found in Keenlyside et al. (2008). Here, we further show that the synchronisation of a 20-year cycle in the subpolar gyre and Nordic Seas leads to SSS positive anomalies that enhance the NAO thermal forcing signal above the deep convection sites. Such positive SSS anomalies in the late 1980s correspond in the real ocean to the comparatively high SSS found between the early 1980s and 1990s, when the negative SSS related to GSAs were propagating in the area (Belkin et al. 1998). In summary, NAO forcing and 20-year cycle initialisation through Mount Agung forcing therefore seem to have conspired with each other to lead to the large AMOC maximum of the 1990s.

Moreover, we argue that GSAs can be seen in this model as a signature of the simulated 20-year cycle. As an alternative to the large sea-ice export from the Arctic proposed by Haak et al. (2003) to explain the 1970s and 1990s GSAs, we argue that changes in the EGC due to local sea-ice cover changes in the Nordic Seas may also play a role and are part of an internal 20-year cycle in the North Atlantic. The model actually succeeds in reproducing the 1970s and 1990s GSAs just through the initialisation of this 20-year cycle by the Mount Agung eruption, and its link with sea-ice cover over the Nordic Seas and EGC. Thus, events similar to the observed GSAs participate in this model to the AMOC variability, as in Häkkinen (1999).

The mechanism evidenced here further support the results of Otterå et al. (2010) suggesting the impact of volcanic eruptions as a pacemaker for internal variability of the AMOC. Here we find that simple initialisation through SST anomaly nudging further improves the timing and amplitude of AMOC variations. An increase of AMOC in response to volcanic eruptions has also been found in other studies (Stenchikov et al. 2009; Zanchettin et al. 2012; Iwi et al. 2012), although Mignot et al. (2011), using an earlier version of the IPSL model, found that such an impact is not systematic and may depend on the state of the ocean at the time of the forcing.

Improved initialisation of the sea ice, and hence salinity at high latitudes, is a thorny issue for prediction systems, but can likely lead to increased predictability. SSS nudging may thus still be needed, especially at high latitude. More work is needed to explore this issue.

The model exhibits large biases in the North Atlantic, with a too weak AMOC, convection sites that are not correctly located and an overestimation of sea ice in the Nordic Seas (Dufresne et al. submitted). The encouraging results we obtain in predicting the AMOC variability are therefore somewhat unexpected. Nevertheless we argue that the agreement between simulations and AMOC reconstructions is due to the basin-scale dynamics, such as advection time scales, which are relatively well captured by the model. Still, we cannot rule out that correct AMOC variations are obtained for wrong reasons namely through error compensations. In particular the air–sea ice interactions in the Nordic Seas remain a weak point of the suite of mechanisms proposed here. Continuous observations of the subpolar gyre and the EGC in particular may help to verify the pertinence of this mechanism.

Finally and as a cautionary note, the decadal prediction system described here should be taken as a methodological set up, since we do not claim it is mature enough to propose any reliable prediction to be used for societal applications.

Acknowledgments We thank Sophie Szopa for providing the external forcing data (Fig. 1). We also thank Jean-Louis Dufresne for fruitful discussions concerning the historical simulations and Sébastien Denvil, Marie-Alice Foujols and Arnaud Caubel for running the historical simulations. We wish to acknowledge the use of the Ferret software for analysis and graphics in this paper and the help of Patrick Brockmann for the use of this software. This research was supported was supported by the "Gestion des Impacts du Changement Climatique" Programme (GICC) under the EPIDOM project funded by MEDDTL (French Minister of Ecology and sustained development). We also acknowledge financial support from the CNRS/INSU/LEFE/EVE French program through the Ti Ammo project. The work presented has largely benefited from the work of our colleagues of the IPSL Climate Modeling Centre. This work benefited of the HPC resources of CCRT and IDRIS made available by GENCI (Grand Equipement National de Calcul Intensif). We also would like to thank the anonymous referees for their constructive and helpful remarks on this manuscript.

References

Álvarez-Garcia F, Latif M, Biastoch A (2008) On multidecadal and quasi-decadal North Atlantic variability. J Clim 21:3433–3452. doi:10.1175/2007JCLI1800.1

Aumont O, Bopp L (2006) Globalizing results from ocean in situ iron fertilization studies. Glob Biogeochem Cycles 20(2):GB2017. doi:10.1029/2005GB002591

Belkin IM (2004) Propagation of the "Great Salinity Anomaly" of the 1990s around the northern North Atlantic. Geophys Res Lett 31:L08306, 4 pp. doi:10.1029/2003GL019334

Belkin IM, Levitus S, Antonov J, Malmberg S-A (1998) Great salinity anomalies in the North Atlantic. Prog Oceanogr 41:1–68

Boer GJ (2004) Long-timescale potential predictability in an ensemble of coupled climate models. Clim Dyn 23:29–44

Booth PW, Matthews SW, Sisson RE (1963) Bali's sacred mountain blows its top. Natl Geogr 124(10):436

Bretherton CS, Smith C, Wallace JM (1992) An intercomparison of methods for finding coupled patterns in climate data. J Clim 5:541–560

Chylek P, Folland CK, Dijkstra KA, Lesins G, Dubey MK (2011) Ice-core data evidence for a prominent near 20 year time-scale of the Atlantic multidecadal oscillation. Geophys Res Lett 38:L13704, 5 pp. doi:10.1029/2011GL047501

Collins M et al (2006) Interannual to decadal climate predictability in the North Atlantic: a multimodel-ensemble study. J Clim 19:1195–1203

Cunningham SA et al (2007) Temporal variability of the Atlantic meridional overturning circulation at 26.5°N. Science 17:935–938

Czaja A, Marshall J (2001) Observations of atmosphere–ocean coupling in the North Atlantic. Q J R Meteorol Soc 127:1893–1916

Delworth TL, Greatbatch RJ (2000) Multidecadal thermohaline circulation variability driven by atmospheric surface flux forcing. J Clim 13:1481–1495

Delworth TL, Manabe S, Stouffer R (1993) Interdecadal variations of the thermohaline circulation in a coupled ocean–atmosphere model. J Clim 6:1993–2011

Deser C, Blackmon ML (1993) Surface climate variations over the North Atlantic Ocean during winter: 1900–1989. J Clim 6:1743–1753

Dijkstra HA, Ghil M (2005) Low-frequency variability of the ocean circulation: a dynamical systems approach. Rev Geophys 43:RG3002. doi:10.1029/2002RG000122

Dunstone NJ, Smith DM (2010) Impact of atmosphere and sub-surface ocean data on decadal climate prediction. Geophys Res Lett 37:L02709. doi:10.1029/2009GL041609

Dufresne J-L, Foujols M-A, Denvil S, Caubel A, Marti O, Aumont O, Balkanski Y, Bekki S, Bellenger H, Benshila R, Bony S, Bopp L, Braconnot P, Brockmann P, Cadule P, Cheruy F, Codron F, Cozic A, Cugnet D, de Noblet N, Duvel J-P, Ethé C, Fairhead L, Fichefet T, Flavoni S, Friedlingstein P, Grandpeix J-Y, Guez L, Guilyardi E, Hauglustaine D, Hourdin F, Idelkadi, Ghattas J, Joussaume S, Kageyama M, Krinner G, Labetoulle S, Lahellec A, Lefebvre M-P, Lefevre F, Levy C, Li Z. X., Lloyd J, Lott F, Madec G, Mancip M, Marchand M, Masson S, Meurdesoif Y, Mignot J, Musat I, Parouty S, Polcher J, Rio C, Schulz M, Swingedouw D, Szopa S, Talandier C, Terray P, Viovy N Climate change projections using the IPSL-CM5 earth system model: from CMIP3 to CMIP5. Clim Dyn (submitted)

Eden C, Jung T (2001) North Atlantic interdecadal variability: oceanic response to the North Atlantic oscillation (1865–1997). J Clim 14:676–691

Escudier R, Mignot J, Swingedouw D A 20-year coupled ocean–sea ice–atmosphere variability mode in the North Atlantic in an AOGCM. Clim Dyn (submitted)

Fichefet T, Maqueda MAM (1997) Sensitivity of a global sea ice model to the treatment of ice thermodynamics and dynamics. J Geophys Res 102:2609–2612

Frankcombe L, von der Heydt A, Dijsktra HA (2010) North atlantic multidecadal climate variability: an investigation of dominant time scales and processes. J Clim 23:3626–3638

Frankignoul C, Kestenare E (2002) The surface heat flux feedback. Part 1: estimates from observations in the Atlantic and the North Pacific. Clim Dyn 19:633–647

Haak H, Jungclaus J, Mikolajewicz U, Latif M (2003) Formation and propagation of great salinity anomalies. Geophys Res Lett 30(9):1473. doi:10.1029/2003GL017065

Häkkinen S (1999) A simulation of thermohaline effects of a great salinity anomaly. J Clim 12:1781–1795

Haney RH (1971) Surface thermal boundary conditions for ocean circulation models. J Phys Oceanogr 1:241–248

Hourdin F et al (2006) The LMDZ4 general circulation model: climate performance and sensitivity to parametrised physics with emphasis on tropical convection. Clim Dyn 27:787–813

Huck T, Colin de Verdière A, Estrade P, Schopp R (2008) Low-frequency variations of the large-scale ocean circulation and heat transport in the North Atlantic from 1955–1998 in situ temperature and salinity data. Geophys Res Lett 35:L23613. doi:10.1029/2008GL035635

Hurrell JW (1995) Decadal trends in the North Atlantic oscillation: regional temperatures and precipation. Science 269:676–679

Iwi AM, Hermanson L, Haines K, Sutton RT (2012) Mechanisms linking volcanic aerosols to the Atlantic meridional overturning circulation. J Clim 25:3039–3051

Kanzow T, Cunningham SA, Johns WE, Hirschi JJ-M, Marotzke J, Baringer MO, Meinen CS, Chidichimo MP, Atkinson C, Beal LM, Bryden HL, Collins J (2010) Seasonal variability of the Atlantic meridional overturning circulation at 26.5°N. J Clim 23:5678–5698. doi:10.1175/2010JCLI3389.1

Keenlyside NS, Latif M, Jungclaus J, Kornblueh L, Roeckner E (2008) Advancing decadal scale climate prediction in the North Atlantic sector. Nature 453:84

Kistler R, Kalnay E, Collins W, Saha S, White G, Woollen J, Chelliah M, Ebisuzaki W, Kanamitsu M, Kousky V, van den Dool H, Jenne R, Fiorino M (2001) The NCEP-NCAR 50-year reanalysis: monthly means CD-ROM and documentation. Bull Am Meteorol Soc 82:247–268

Knight J, Allan R, Folland C, Vellinga M, Mann M (2005) A signature of persistent natural thermohaline circulation cycles in observed climate. Geophys Res Lett 32:L20708. doi:10.1029/2005GL024233

Köhl A, Stammer D (2008) Variability of the meridional overturning in the North Atlantic from the 50-year GECCO state estimation. J Phys Oceanogr 38(9):1913–1930. doi:10.1175/2008JPO3775.1

Latif M, Roeckner E, Botzet M, Esch M, Haak H, Hagemann S, Jungclaus J, Legutke S, Marsland S, Mikolajewicz U, Mitchell J (2004) Reconstructing, monitoring, and predicting multidecadal-scale changes in the North Atlantic thermohaline circulation with sea surface temperature. J Clim 17(7):1605–1614

Latif M, Collins M, Pohlmann H, Keenlyside N (2006) A review of predictability studies of the Atlantic sector climate on decadal time scales. J Clim 19:5971–5987

Levitus S, Antonov JI, Boyer TP, Locarnini RA, Garcia HE, Mishonov AV (2009) Global ocean heat content 1955–2008 in light of recently revealed instrumentation problems. Geophys Res Lett 36:L07608. doi:10.1029/2008GL037155

Lherminier P, Mercier H, Huck T, Gourcuff C, Perez FF, Morin P, Kermabon C (2010) The meridional overturning circulation and the subpolar gyre observed at the A025-OVIDE section in June 2002 and 2004. Deep-Sea Res I 57:1374–1391. doi:10.1016/j.dsr.2010.07.009

Luo JJ, Masson S, Behera S, Shingu S, Yamagata T (2005) Seasonal climate predictability in a coupled OAGCM using a different approach for ensemble forecasts. J Clim 18:4474–4497

Madec G (2008) NEMO ocean engine. Note du Pole de modélisation, Institut Pierre-Simon Laplace (IPSL), France, no. 27, ISSN no: 1288-1619

Madec G, Delecluse P (1997) The OPA/ARPEGE and OPA/LMD global ocean–atmosphere coupled model. Int WOCE Newslett 26

Mignot J, Frankignoul C (2005) The variability of the Atlantic meridional overturning circulation, the North Atlantic oscillation, and the El Nino Southern oscillation in the Bergen climate model. J Clim 18(13):2361–2375. doi:10.1175/JCLI3405.1

Mignot J, Khodri M, Frankignoul C, Servonnat J (2011) Volcanic impact on the Atlantic ocean over the last millennium. Clim Past 7:1439–1455. doi:10.1007/s00382-012-1466-1

Msadek R, Frankignoul C (2009) Atlantic multidecadal oceanic variability and its influence on the atmosphere in a climate model. Clim Dyn 33:45–62. doi:10.1007/s00382-008-0452-0

Msadek R, Dixon K, Delworth T, Hurling W (2010) Assessing the predictability of the Atlantic meridional overturning and associated fingerprints. Geophys Res Lett 37:L19608. doi: 10.1029/2010GL044517

Otterå OH, Bentsen M, Drange H, Suo L (2010) External forcing as a metronome for Atlantic multidecadal variability. Nat Geosci 3:688–694. doi:10.1038/ngeo955

Pohlmann H et al (2004) Estimating the decadal predictability of a coupled AOGCM. J Clim 17:4463–4472

Pohlmann H, Jungclaus J, Köhl A, Stammer D, Marotzke J (2009) Initializing decadal climate predictions with the GECCO oceanic synthesis: effects on the North Atlantic. J Clim 22:3926–3938

Persechino A, Mignot J, Swingedouw D, Labetoule S, Guilyardi E Decadal predictability of the Atlantic meridional overturning circulation and climate in the IPSL-CM5A model. Clim Dyn (submitted)

Peterson LC, Haug GH, Hughen KA, Rohl U (2000) Rapid changes in the hydrologic cycle of the tropical North Atlantic during the last glacial. Science 290:1947–1951

Rayner NA, Parker DE, Horton EB, Folland CK, Alexander LV, Rowell DP, Kent EC, Kaplan A (2003) Global analyses of sea surface temperature, sea ice, and night marine air temperature since the late nineteenth century. J Geophys Res 108(D14):4407. doi:10.1029/2002JD002670

Reynolds RW, Smith TM, Liu C, Chelton DB, Casey KS, Schlax MG (2007) Daily high-resolution blended analyses for sea surface temperature. J Clim 20:5473–5496

Sicre M-A, Jacob J, Ezat U, Rousse S, Kissel C, Yiou P, Eiríksson J, Knudsen KL, Jansen E, Turon J-L (2008) Decadal variability of sea surface temperatures off North Iceland over the last 2000 years. Earth Planet Sci Lett 268:137–142

Smith TM, Reynolds RW, Peterson TC, Lawrimore J (2008) Improvements to NOAA's historical merged land-ocean surface temperature analysis (1880–2006). J Clim 21:2283–2296. doi: 10.1175/2007JCLI2100.1. http://dx.doi.org/

Stenchikov G, Delworth TL, Ramswamy V, Stouffer RJ, Wittenberg A, Zeng F (2009) Volcanic signals in oceans. J Geophys Res 114:D16104. doi:10.1029/2008JD011673

Stouffer RJ, Yin J, Gregory JM, Dixon KW, Spelman MJ, Hurlin W, Weaver AJ, Eby M , Flato GM, Hasumi H, Hu A, Jungclaus JH, Kamenkovich IV, Levermann A, Montoya M, Murakami S, Nawrath S, Oka A, Peltier WR, Robitaille DY, Sokolov A, Vettoretti G, Weber SL (2006)Investigating the causes of the response of the thermohaline circulation to past and future climate changes. J Clim 19:1365–1387

Sundby S, Drinkwater K (2007) On the mechanisms behind salinity anomaly signals of the northern North Atlantic. Prog Oceanogr 73:190–202

Swingedouw D, Mignot J, Braconnot P, Mosquet E, Kageyama M, Alkama R (2009) Impact of fresh water release in the North Atlantic under different climate conditions in an OAGCM. J Clim 22:6377-6403

Taylor KE, Stouffer RJ, Meehl GA (2012) An overview of CMIP5 and the experiment design. Bull Am Meteorol Soc 93:485–498. doi:10.1175/BAMS-D-11-00094.1

Timmermann A, Latif M, Voss R, Grotzner A (1998) North Atlantic interdecadal variability: a coupled air–sea mode. J Clim 11:1906–1932

Timmermann R, Goosse H, Madec G, Fichefet T, Ethe C, Duliere V (2005) On the representation of high latitude processes in the ORCA–LIM global coupled sea ice–ocean model. Ocean Model 8(1–2):175. doi:10.1016/j.ocemod.2003.12.009

Tulloch R, J Marshall (2012) Exploring mechanisms of variability and predictability of Atlantic meridional overturning circulation in two coupled climate models. J Clim 25:4067–4080. doi: 10.1175/JCLI-D-11-00460.1

van Oldenborgh GJ, Doblas-Reyes FJ, Wouters B, Hazeleger W (2012) Skill in the trend and internal variability in a multi-model decadal prediction ensemble. Clim Dyn 38(7):1263–1280. doi: 10.1007/s00382-012-1313-4

Zanchettin D, Timmreck C, Graf H-F, Rubino A, Lorenz S, Lohmann K, Krueger K, Jungclaus JH (2012) Bi-decadal variability excited in the coupled ocean–atmosphere system by strong tropical volcanic eruptions. Clim Dyn 39(1–2):419–444. doi: 10.1007/s00382-011-1167-1

Zhang R, Delworth TL (2006) Impact of Atlantic multidecadal oscillations on India/Sahel rainfall and Atlantic hurricanes. Geophys Res Lett 33:L17712. doi:10.1029/2006GL026267

Zhang S, Rosati A, Harrison MJ (2009) Detection of multi-decadal oceanic variability by ocean data assimilation in the context of a "perfect" coupled model. J Geophys Res 14:C12018. doi: 10.1029/2008JC005261